Cell, Volume *130*

Supplemental Data

SCRAPPER-Dependent Ubiquitination of Active Zone Protein RIM1 Regulates Synaptic Vesicle Release

Ikzuko Yao, Hiroshi Takagi, Hiroshi Ageta, Tomoaki Kahyo, Showbu Sato, Ken Hatanaka, Yoshiyuki Fukuda, Tomoki Chiba, Nobuhiro Morone, Shigeki Yuasa, Kaoru Inokuchi, Toshihisa Ohtsuka, Grant R. MacGregor, Keiji Tanaka, and Mitsutoshi Setou

SUPPLEMENTAL EXPERIMENTAL PROCEDURES

Identification of SCRAPPER and cloning of the *Scrapper* gene

We screened the human genome for genes whose coding sequence contained an F-box domain (characteristic of E3 ligases), a membrane targeting sequence, and whose promoter region contained both a neuron-restrictive silencing element (NRSE) and a cAMP-response element (CRE) within 3-kb upstream of exon 1 from eleven hundred thirty genes using the Celera Discovery System (a search program that is no longer available).

We searched the sequence "TtcagcaccNcggacagcNc" as NRSE and "TGACGTCA" as CRE. In the human *SCRAPPER* promoter sequence, NRSE positions at 721-bp upstream of exon 1 and CRE at 448-, 478-, 1053-, and 2529-bp. In the mouse *scrapper* promoter sequence, NRSE positions at 658-bp upstream of exon 1 and CRE at 853-, 1182-, and 1303-bp. We verified the information at http://www.gene-regulation.com/cgi-bin/pub/programs/match/bin/match.cgi

The F-box domain was identified by the Pfam program. Cloning of the *Scrapper* gene was performed by RT-PCR, using cDNA from newborn mouse brain and *Scrapper*-specific primers. The NCBI accession No. of *scrapper* is 918964.

Antibodies

The rabbit anti-SCRAPPER antibody was raised against the product of pET41-SCRAPPER-LRR containing the amino residues 321-380 of the *Scrapper* coding region. The antibodies used in these experiments include mouse monoclonal antibodies against synaptophysin (Chemicon), Munc13, RIM, CASK, Rab3, SNAP-25, synaptotagmin, synaptogyrin, Rabphillin, Munc18 (BD biosciences), tubulin, actin, MAP2, FLAG (Sigma), Myc (BIOMOL), PSD-95/SAP90 clone K28/42, Cullin1 (Upstate Biotechnology), CREB, p-CREB (Cell Signaling), Skp1, Skp2 (Zymed), GFP, MBP, and Ubiquitin (MBL). Secondary antibodies labeled with horseradish peroxidase or fluorescein were obtained from Jackson Laboratory Inc. and Invitrogen Inc., respectively.

Plasmid Construction

Vectors were constructed by conventional molecular biology techniques. pET41-SCRAPPER-LRR includes 321-380 residues of SCRAPPER. FLAG-scrapper was linked to a pCMV-tag2 vector (Stratagene) and GFP-tagged SCRAPPER to a pEGFPC vector (Clontech).

***In situ* Hybridization for *Scrapper* mRNA**

In situ hybridization was performed essentially as described (Ikegami et al., 2006). The mice were fixed by cardiac perfusion with 4% PFA in 0.1 M Phosphate Buffer (PB) (pH 7.4). The brain was equilibrated in Phosphate Buffered Saline (PBS) consisting of 25% sucrose and embedded in O.C.T. compound (Sakura). The frozen samples were cut with a cryostat into 10 μm and mounted onto glass slides. Hybridization was performed overnight at 65 °C with digoxigenin-labeled RNA probes. Signal detection was done by incubation with alkaline phosphatase-conjugated anti-digoxigenin antibody (diluted to 1:1000; Roche) followed by a coloring reaction in NTMT solution (100 mM Tris-HCl pH 9.5, 100

mM NaCl, 50 mM MgCl, 0.1% Tween 20) containing 35 mg/ml nitro blue tetrazolium (Roche), 17.5 mg/ml 5-bromo-4-chloro-3-indlyl phosphate (Roche), and 2 mM levamisol.

Subcellular Fractionation

Subcellular fractionation of the mouse brain was performed as previously described (Hirao et al., 1998; Yao et al., 1999), and each fraction was kept and analyzed by the western blot technique. Scrapper was in membrane fractions, especially in the SPM (the synaptosomal membrane fraction) and the 0.5% (w/v) Triton X-100-soluble fraction of the SPM. Rab3, PSD-95, and actin served as controls. Homo, the homogenate fraction; P1, the nuclear pellet fraction; S1, the crude synaptosomal fraction; S2, the synaptosomal cytosol fraction; P2, the crude synaptosomal pellet fraction; LP1, the lysed synaptosomal membrane fraction; LP2, the crude synaptic vesicle fraction; SPM, the SPM fraction; sup, the 0.5% (w/v) or 1% (w/v) Triton X-100-soluble fraction of the SPM; ppt, the 0.5% (w/v) or 1% (w/v) Triton X-100-insoluble fraction of the SPM; myelin, the axonal myelin fraction; Mitochondria, the mitochondrial membrane fraction.

Cell Culture and Hippocampal Neuron Culture

HEK293T cells were cultured in DMEM supplemented with 10% FBS and were maintained at 37 °C and 10% CO_2. DNA transfection was by Lipofectamine2000 (Invitrogen). Hippocampal neurons were prepared as described (Kato et al., 2001) with some modifications. In short, the hippocampi were dissected and incubated in a papain solution. The cells were gently triturated and washed with Minimum Essential Medium (MEM) supplemented with 5% horse serum and 5% fetal bovine serum. The cells were plated onto poly-**L**-lysine coated glass cover slips. The culture medium was replaced with

MEM supplemented with B-27 and 0.5 mM glutamine. Cultured cells were transfected with 1 μg DNA with Lipoofectamine2000.

Scrapper Knockout Mice

We used homologous recombination in embryonic stem (ES) cells to generate a disrupted *Scrapper*. Exon 3 (which encodes the region including the F-box domain) and a part of exon 4 (a recombination that generates a frame shift) were replaced by Neo and followed by DT-A for negative selection. Recombinant phages containing the mouse *Scrapper* locus were isolated from a 129/Sv FixII-phage genomic library (Stratagene) using *Scrapper* cDNA as a probe. The genomic structure of the *Scrapper* genomic clones containing exon 2 and four exons from 4 to 7 was analyzed by restriction mapping and sequencing. The gene-targeting vector was constructed using a 7.4-kb fragment downstream from the SpeI site and a 5.8-kb fragment upstream from the NdeI site for the 5' and 3' flanking homologous regions, respectively. A neo cassette and an SV40 polyadenylation signal from pMC1Neo PolyA (Stratagene) were introduced by the NcoI and HindIII sites at the 5’ and 3’ ends, respectively. A 3.2-kb segment containing exon 2 between the flanking regions was replaced by the neo cassette and was subcloned into pBluescript, resulting in a deletion of the exons encoding most of the F-box domain of Scrapper. A diphtheria toxin A (DT-A) expression cassette was inserted at the 3' end of the genomic DNA for negative selection. The targeting construct was linearized by SpeI digestion. E14TG2a ES cells were electroporated with a SpeI-linearized targeting vector and selected in G418. The targeted clones were confirmed by Southern blot analysis of 1) KpnI-HindIII-digested genomic DNA probed with a 750 bp fragment downstream of the KpnI site and upstream of the 5' of the targeting construct, and of 2) NcoI-digested genomic DNA probed with an 800 bp fragment between the NdeI and the NcoI sites at the 3' end. Heterozygous ES cells were

injected into blastocysts of C57BL/6J strain mice to generate germ-line chimeras. Chimeric males were mated with C57BL/6J females, and subsequent experimental procedures were performed on a mixed background. Genotypes were determined by Southern blotting as described above, or by PCR using the following three primers: SCR-KO-3', 5'-CCTCAATGTCCCTCTGGAAATC-3'; SCR-KO-5', 5'-CGGAGACTGAGGACATTTTTGG-3'; and SCR-KO-Neo, 5'-TGCATCTGCGTGTTCGAATTCG-3'.

The WT and mutant alleles produce 0.2- and 0.3-kb products respectively in PCR genotyping. Western analysis using anti-SCRAPPER antibody indicated the disappearance of SCRAPPER in the brain of the homozygote (see Fig. 3A).

Every analysis of SCR-KO mice was performed on littermates derived from mating heterozygous mutant mice on a hybrid SV129/C57B6 background, and was confirmed with several independent litters derived from many generations of heterozygous breeding. Note that SCR-KO homozygotes which had been back-crossed to pure C57BL/6J background exhibited postnatal lethality at postnatal day 1 (+/+, 61; +/-, 133; -/-, 6), while many were born alive (+/+, 64; +/-, 141; -/-, 32).

Scrapper Transgenic Mice

We established three independent mouse lines over-expressing EGFP-fused SCRAPPER (TG-22, TG-26 TG-31). The EGFP-SCRAPPER transgene contains a CaMKII promoter, an EGFP tag, a *Scrapper*-coding region, and a polyadenylation (poly A) signal. *Scrapper* cDNA encoding amino acids 1-438 was cloned into pEGFPC2 (BD clontech), and the restriction enzyme sites (AscI-FseI) were attached by PCR. MM403, which contains a 8.5-kb mouse CaMKII promoter and was kindly provided by Dr. Kida (Mayford et al., 1996), was modified by the insertion of AscI-FseI sites and a polyA signal into the NotI site (CaMPolyA plasmid). Then EGFP-SCRAPPER was cloned into the AscI-FseI sites of

CaMPolyA. All cloning junctions were verified by DNA sequencing. The EGFP-SCRAPPER transgene construct was excised from MM403 using SfiI sites and was purified using the EndoFree Plasmid Kit (Qiagen, Hilden, Germany). The 11-kb transgene was isolated by agarose gel electrophoresis, electroeluted, and purified using Gelase (EPICENTRE G09050). The founder mice and offspring were identified by Southern blot and PCR analysis using two independent transgene-specific probes and primers. Southern blot analysis of genomic DNA from hemizygous mice of indicated TG-lines probed with polyA signal sequence indicate that the copy numbers varied according to the mouse line. Transgene products were detected using anti-SCRAPPER antibody (see Fig. 3B).

Quantification of Fluorescent Images

For the quantitative analyses of signal intensity of RIM in the SCR-KO and SCR-TG, the confocal fluorescent images from the brain sections or the cultures were analyzed. In the cultured neuron analyses, signal intensities from 3,000 synapses were measured for one experiment for WT and KO. The experiments were independently repeated three times and the results were averaged. The image was analyzed with Adobe Photoshop 8.0, NIH Image 1.61, and Image-J, and Stat View 4.0.

Transmission Electron Microscope Observation

Adult mice were perfused transcardially with a solution of 2% paraformaldehyde and 2.5% glutaraldehyde in 0.1 M phosphate buffered saline (PBS, pH 7.4). The brains were removed and coronal sections (100 μm in thickness) were prepared on a vibratome. The sections were treated with 1% osmium tetroxide in PBS, and dehydrated with an ascending series of ethanol (up to 100%). Dehydrated specimens were substituted in propylene oxide, and then embedded in EPON 812 resin (TAAB Laboratories Equipment Ltd., UK). The brocks were

cut with an ultramicrotome (Ultracut UCT, Leica, Wien, Austria), collected on copper slot grids, stained with uranyl acetate / lead citrate, and then observed with a transmission electron microscope (JEM-1230, JEOL, Tokyo, Japan). The quantitative analysis of synapses to the apical dendrites in the distal stratum radiatum of the hippocampal CA1 region synapse density (per 100 μm^2) was determined on the basis of post synaptic densities (PSDs) per area from randomly selected low-magnification EM micrographs from three WT and three SCR-KO mice. The size of the Active Zone (AZ) (nm) was determined as the extension or the PSD. The synaptic vesicles cluster density was determined by the SV density in the resting pools. Analysis was performed as described previously (Altrock et al., 2003; Schoch et al., 2002).

RNA Interference Experiment

RIM1 was knockdowned by the miR-RNAi system (Invitrogen). For the RIM1 RNAi construct, we used The BLOCK-iT RNAi Designer (Invitrogen) and selected "GTGGTTATGTGGGTATGCAAT" (RIM1_538) as a target sequence, and annealed the following oligonucleotides and inserted in cloning site of miR-RNA vector :
5'-TGCTGATTGCATACCCACATAACCACGTTTTGGCCACTGACTGACGTGGTTA TGGGTATGCAAT-3'; and
5'-CCTGATTGCATACCCATAACCACGTCAGTCAGTGGCCAAAACGTGGTTATGT GGGTATGCAATC-3'. We used "TAGTGTCAAAGTATGGGGTTA" (Random) as a control, which is no homology to all genes in human and mouse genome. We used Lipofectamine2000 (Invitrogen) for the transfection of miR-RNA plasmid. The efficiency of knock down was checked by co-transfection with Myc tagged RIM1 to 293T cells.

Recording of mEPSC

AMPA-receptor-mediated mEPSC was recorded as described previously (Inoue et al., 2006). Briefly, culture medium was exchanged for a saline solution containing 168 mM NaCl, 2.4 mM KCl, 2 mM $CaCl_2$, 1 mM $MgCl_2$, 10 mM **D**-glucose, 10 mM HEPES, and 0.5 μM TTX (pH 7.3). Electrodes (2 - 4 MΩ) were filled with the whole-cell pipette solution containing 120 mM K-acetate, 20 mM KCl, 0.1 mM $CaCl_2$, 5 mM $MgCl_2$, 0.2 mM EGTA, 5mM ATP, and 10 mM HEPES (pH 7.3). A whole-cell recording configuration was achieved from the GFP-expressing neurons using an EPC-7 amplifier (HEKA, Germany) and a Digidata 1200 acquisition board (Axon Instruments). Membrane potential was clamped at -70 mV, and the signals were filtered at 10 kHz with gain set at 0.5 mV/ pA for 40-sec recording periods. In all instances, cells were excluded from analysis if a leak current >200 pA was observed. Membrane resistance (R_m), series resistance (R_s), and membrane capacitance (C_m) were monitored. Only recordings with R_m >120 MΩ and R_s <15 MΩ were included in the analysis. (Note that mean R_m, R_s, and C_m were not different ($p > 0.05$) among or within cells in which comparisons were made; CNQX (50 μM), an AMPA receptor antagonist, was bath-applied during a subset of recordings to determine that detected mEPSC events were AMPA-receptor-mediated.) Measurements of the frequency and amplitude of mEPSC were performed for a period of 40 sec. mEPSCs were detected by setting the amplitude threshold to three times the background noise level. In all electrophysiological experiments, a similar amount of data was acquired from GFP-expressing neurons on the same day. To arrive at the normalized values, the average frequency and amplitude of mEPSC events were determined for each recorded neuron. The average frequency (Hz), amplitude (pA), rise time (ms), and decay time (ms) from each neuron were then averaged to give a value for the entire population. Statistical significance was determined by a Student's *t*-test (two-tailed). The variable *n* corresponds to the number of neurons tested. This methodology was applied to all subsequent mEPSC plots. * $p < 0.05$ was considered to be statistically significant. All electrophysiological experiments were

performed using at least three different platings of neurons from two different transfections.

Electrophysiology of Hippocampal Slices

Hippocampal slices were prepared from ether-anesthetized 3- to 4-week-old SCR-KO mice. Mice were decapitated and the brain was rapidly removed and placed in ice-cold high-sucrose solution (HS) containing 250 mM sucrose, 3.5 mM KCl, 26 mM $NaHCO_3$, 10 mM **D**-glucose, 1.3 mM NaH_2PO_4, 1.2 mM $MgSO_4$, and 3.8 mM $MgCl_2$. Transverse 300-μm-slices were prepared with a microslicer (PRO7, Dosaka EM, Kyoto, Japan) and then incubated for at least 120 min at room temperature in a normal solution (NS) containing 125 mM NaCl, 3.5 mM KCl, 26 mM $NaHCO_3$, 10 mM **D**-glucose, 1.3 mM NaH_2PO_4, 1.2 mM $MgSO_4$, 3.8 mM $MgCl_2$, and 2.5 mM $CaCl_2$. For recording, 300-μm-thick slices of mouse hippocampus were maintained at 30 °C in a recording chamber perfused with a modified NS containing 124 mM NaCl, 3.5 mM KCl, 26 mM $NaHCO_3$, 1.3 mM NaH_2PO_4, 1.2 mM $MgSO_4$, 2 mM $CaCl_2$ and 10 mM **D**-glucose. All solutions were saturated with a 95% O_2/5% CO_2 gas mixture throughout the experiment. Field excitatory postsynaptic potentials (fEPSPs) were recorded either from the outer dendritic region of CA1 while stimulation was performed at the same level in the stratum radiatum, close to the pyramidal cells; stimulation was performed with monopolar glass electrodes, and recording was done with ACSF-filled glass pipettes (<2 MΩ). Test stimuli consisted of biphasic 100 μsec pulses of constant current delivered by stimulus isolation units. The stimulus intensity was then adjusted to evoke a test response that was ~50% of the maximal signal amplitude (WT and KO mice, respectively); typically, this resulted in stimulation intensities of 40-50 mA. Paired-pulse facilitation (PPF) was measured by using a two-paired 50, 100, 200, 300,and 400-ms interpulse interval stimulus. The PPF ratio (2^{nd} fEPSP slope/ 1^{st} fEPSP slope) was evaluated in each inter-pulse interval (IPI). Basal

synaptic transmission was monitored by alternating, low-frequency stimulation (every 60 sec). Baseline responses had to be stable for at least 30 min before these stimuli were delivered. mEPSC was recorded from the soma of CA1 pyramidal neuron under the voltage clamp conditions in the 0.5 μM TTX containing NS (HP=-70mV). Picrotoxin (100 μM) and APV (100 μM) were added to the 0.5 μM TTX containing NS to prevent the $GABA_A$-receptor-mediated mIPSC and NMDA-receptor-mediated mEPSC. The signals were amplified with an amplifier (EPC-7, HEKA, Germany). fEPSPs and mEPSC were digitized (1 kHz) using the acquisition system pClamp6 and stored on magnetic media, and the fEPSP slope was analyzed off-line using the analysis system Clampfit 8.0 (Axon Instruments).

SUPPLEMETAL REFERENCES

Altrock, W.D., tom Dieck, S., Sokolov, M., Meyer, A.C., Sigler, A., Brakebusch, C., Fassler, R., Richter, K., Boeckers, T.M., Potschka, H.*, et al.* (2003). Functional inactivation of a fraction of excitatory synapses in mice deficient for the active zone protein bassoon. Neuron *37*, 787-800.

Hirao, K., Hata, Y., Ide, N., Takeuchi, M., Irie, M., Yao, I., Deguchi, M., Toyoda, A., Sudhof, T.C., and Takai, Y. (1998). A novel multiple PDZ domain-containing molecule interacting with N-methyl-D-aspartate receptors and neuronal cell adhesion proteins. J Biol Chem *273*, 21105-21110.

Ikegami, K., Mukai, M., Tsuchida, J., Heier, R.L., MacGregor, G.R., and Setou, M. (2006). TTLL7 is a mammalian beta-tubulin polyglutamylase required for growth of MAP2-positive neurites. J Biol Chem *281*, 30707-30716.

Inoue, E., Mochida, S., Takagi, H., Higa, S., Deguchi-Tawarada, M., Takao-Rikitsu, E., Inoue, M., Yao, I., Takeuchi, K., Kitajima, I.*, et al.* (2006). SAD: A Presynaptic

Kinase Associated with Synaptic Vesicles and the Active Zone Cytomatrix that Regulates Neurotransmitter Release. Neuron *50*, 261-275.

Kato, A., Fukuda, T., Fukazawa, Y., Isojima, Y., Fujitani, K., Inokuchi, K., and Sugiyama, H. (2001). Phorbol esters promote postsynaptic accumulation of Vesl-1S/Homer-1a protein. Eur J Neurosci *13*, 1292-1302.

Mayford, M., Bach, M.E., Huang, Y.Y., Wang, L., Hawkins, R.D., and Kandel, E.R. (1996). Control of memory formation through regulated expression of a CaMKII transgene. Science *274*, 1678-1683.

Schoch, S., Castillo, P.E., Jo, T., Mukherjee, K., Geppert, M., Wang, Y., Schmitz, F., Malenka, R.C., and Sudhof, T.C. (2002). RIM1alpha forms a protein scaffold for regulating neurotransmitter release at the active zone. Nature *415*, 321-326.

Yao, I., Hata, Y., Hirao, K., Deguchi, M., Ide, N., Takeuchi, M., and Takai, Y. (1999). Synamon, a novel neuronal protein interacting with synapse-associated protein 90/postsynaptic density-95-associated protein. J Biol Chem *274*, 27463-27466.

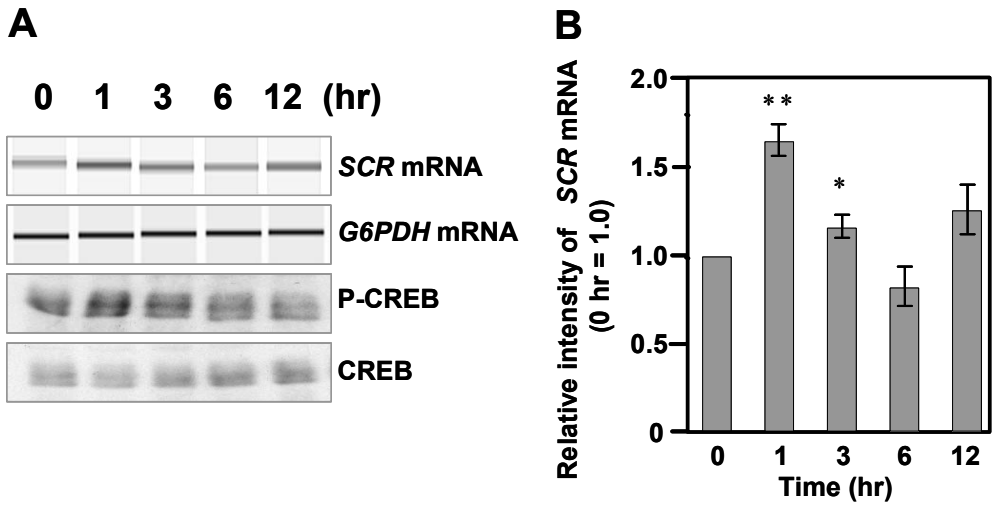

Fig. S1 Increased steady-state level of *Scrapper* mRNA (*SCR* mRNA) after forskolin stimulation.

Cyclic-AMP responsive expression of *Scrapper* mRNA was observed in primary culture of hippocampal neurons 1 hr following induction by forskolin (a cAMP signaling activator)

(A) mRNA from cultured neurons was analyzed by RT-PCR and (B) relative expression levels quantified using a 2100 Bioanalyzer (Agilent). *G6PDH* mRNA was used as an internal control for starting template. Relative ratio of phospho-CREB (P-CREB), and non-phosphorylated CREB (CREB) protein was used to verify stimulation by forskolin (50 μM). Data are expressed as means ± SEM (n=4). Statistical significance was determined by Student's t-test (** $p < 0.01$, * $p < 0.05$).

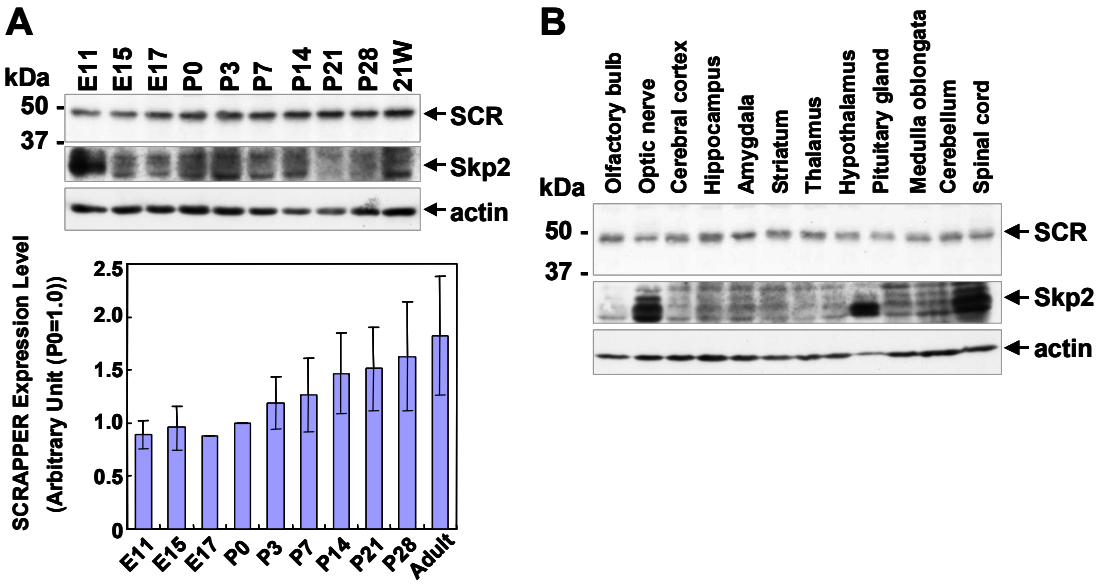

Fig. S2 Expression of SCRAPPER protein in mouse brain.

(A) Western analysis of levels of SCRAPPER (SCR) in the mouse brain revealed a gradual increase with age, from midgestation to adult. The signal intensity of SCRAPPER protein at P0 was used as an arbitrary reference level (1.0). (B) Western blot analyses of SCRAPPER in specific regions of mouse brain. In adult mice, highest levels of SCRAPPER were observed in the brain (Fig. 1A) where it appeared evenly distributed. Ten-μg protein was applied to each lane. Skp2 and actin served as loading controls. Data are expressed as means ± SEM (n=3).

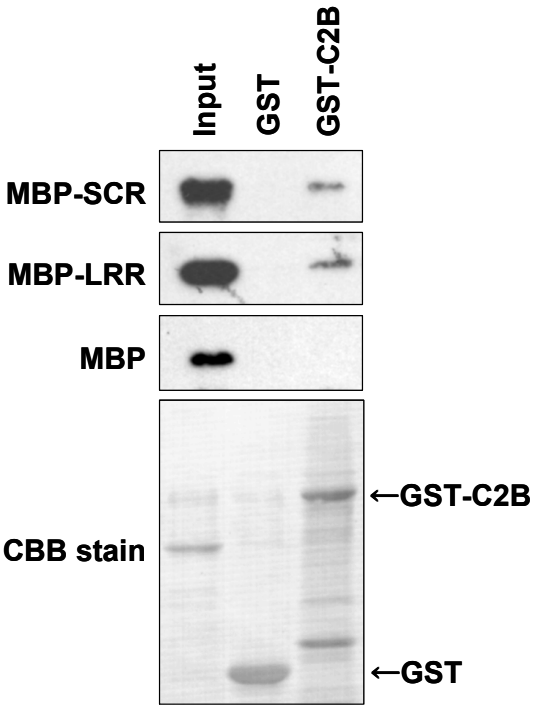

Fig. S3 Direct binding of SCRAPPER to C2B domain of RIM1.

Purified recombinant SCRAPPER and C2B domain of RIM1 directly interacted in an *in vitro* pull-down assay. Bacterially expressed and purified MBP-tagged SCRAPPER (MBP-SCR) or -SCRAPPER LRR domains (MBP-LRR) was pulled down with GST-tagged C2B domain of RIM1 (GST-C2B) fixed on Glutathione-Sepharose, and then detected with anti-MBP antibody. The bottom panel shows the representative CBB (Coomassie Brilliant Blue)-stained pattern of GST and GST-C2B proteins.

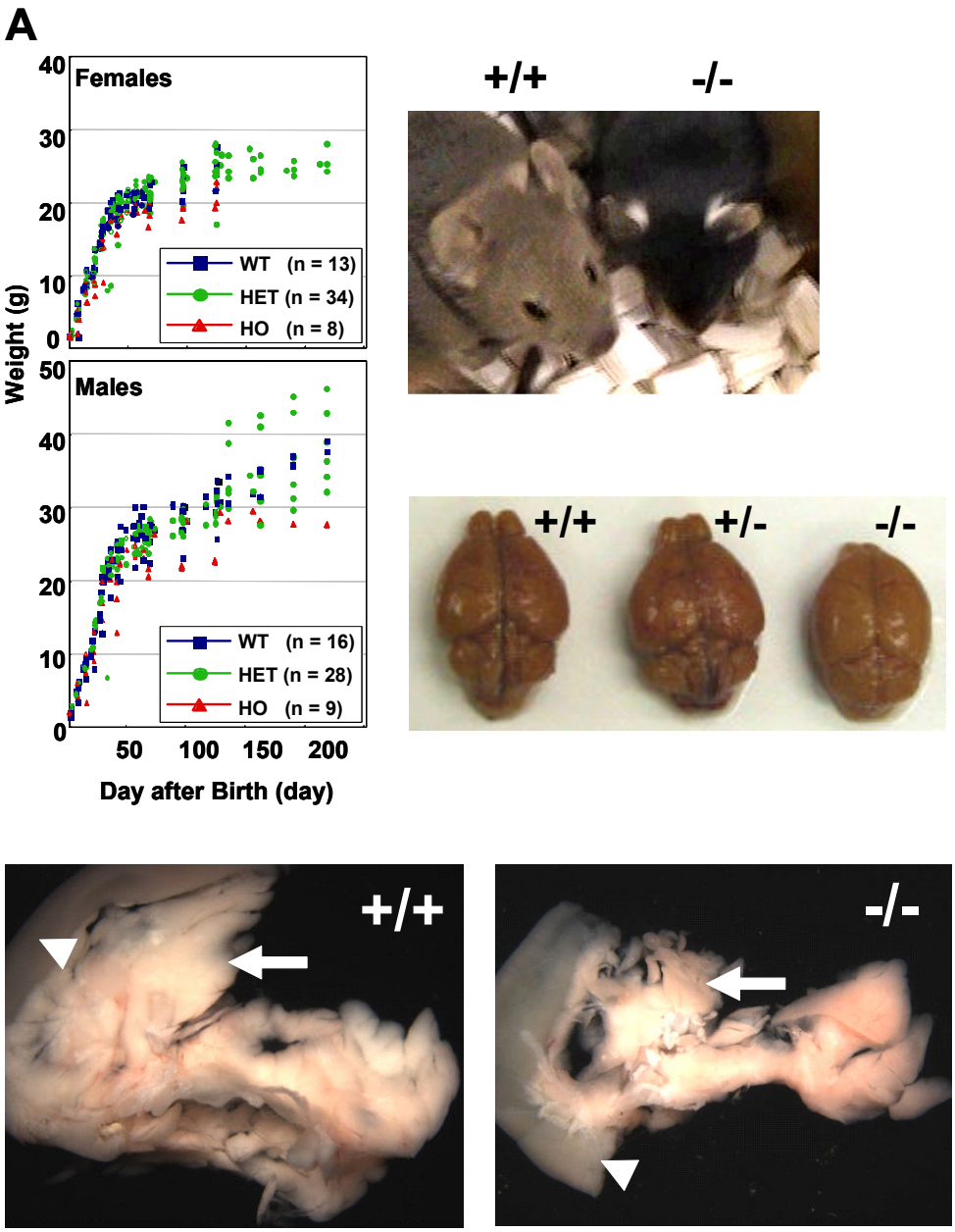

Fig. S4 *Scrapper*-knockout (SCR-KO) mice display reduced body mass and smaller pancreas.

(A) Body weight of *Scrapper* wild type (WT), heterozygous (HET) and homozygous (HO) mutant mice at different ages. Photographs of (B) mice, (C) brains, and (D) pancreas (arrow) and duodenum (arrowhead) in *Scrapper* wild type (+/+), heterozygous (+/-) and homozygous (-/-) mutant mice. The smaller pancreas in SCR-KO mice suggests that SCRAPPER functions not only in CNS but also other tissues.

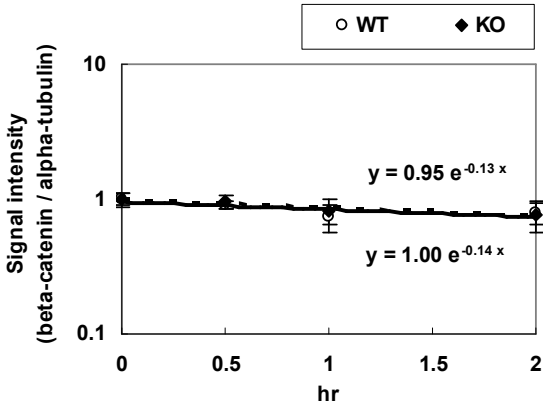

Half-life (hr)		
	RIM1	beta-catenin
WT	0.7±0.1	5.4±0.3
SCR-KO	5.0±0.1	5.0±0.1
SCR-KO/WT	7.1	0.9

Fig. S5 Analysis of half-life of RIM1 by exponential curve fitting.

The half-life of beta-catenin (and RIM1, Fig 3H) protein in WT or SCR-KO neuron was calculated from the result of western blotting densitometry by exponential curve fitting. Protein half-life was normalized to alpha-tubulin, which undergoes slow turn over, and whose amount is known to be unaffected in SCR-KO. The data within 1 hr, the period during which RIM1 decreased linearly, were used for analysis. The values in the graph show the average signal intensity from three experiments. The broken and solid lines show the estimated trend lines of WT and SCR-KO, respectively. Data are expressed as means ± SEM (n=4).

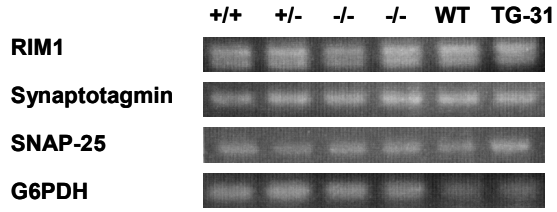

Fig. S6 Steady-state levels of mRNA of RIM1, Synaptotagmin, and SNAP-25 were unaffected by changes in the level of SCRAPPER in the brain.

The level of mRNA for presynaptic proteins such as RIM1, synaptotagmin, and SNAP-25 were unchanged in SCR-TG, SCR-KO, and WT mice. mRNA from the brains of *Scrapper*-knockout and transgenic mice was analyzed by RT-PCR. The amounts of PCR products were estimated by comparing the intensity of their signals.
(+/+): *Scrapper*-wild type; (+/-): *Scrapper*-heterozygous; (-/-): *Scrapper*-homozygous;
WT: non-transgenic mouse, and TG-31: *Scrapper* transgenic mouse.

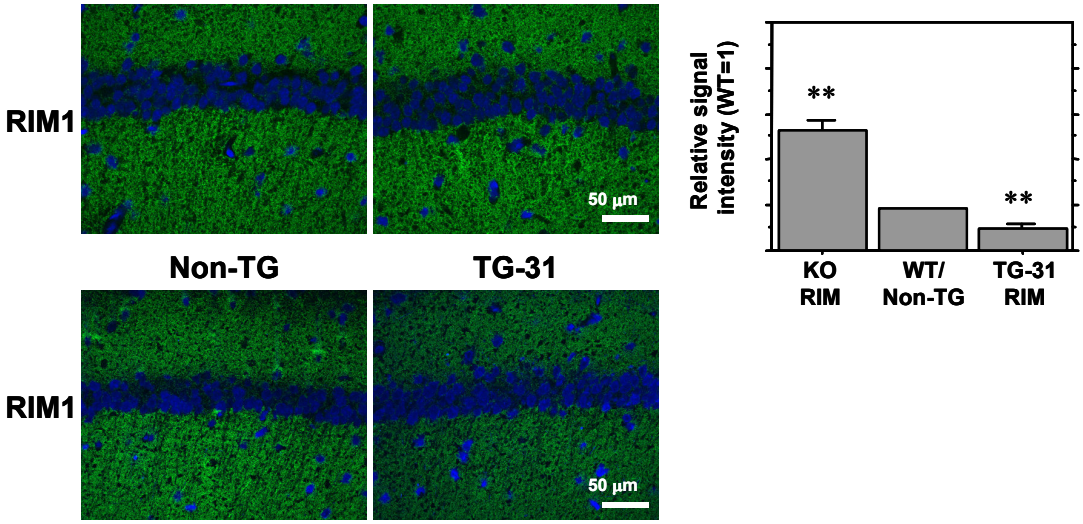

Fig. S7 Increased steady-state RIM1 in synaptic layer of SCR-KO mice.

Immunofluorescence analyses of SCR-KO hippocampi revealed that the increased level of RIM1 occurred in the synaptic region, not in the cell-body. Conversely, the intensity of RIM-specific fluorescence in the synaptic region was reduced in SCR-TG hippocampi relative to that of WT. (A) Immunofluorescence of hippocampal sections from wild type (+/+ or Non-TG), SCR-KO (-/-) and SCR-TG (TG-31) littermate animals were labeled with the RIM antibody (green) and TOTO-3 (blue). (B) Quantitative analysis of the signals at synaptic layer in A compared to those of WT. Quantities are indicated relative to the RIM protein signal in WT mice. Error bars show SEM (n=3). The intensity of RIM was significantly increased in the SCR-KO and decreased in the SCR-TG mice compared to the WT/Non-TG mice (** $p < 0.001$, statistical analyses were by the Student's t-test). +/+, wild-type; -/-, SCR-KO.

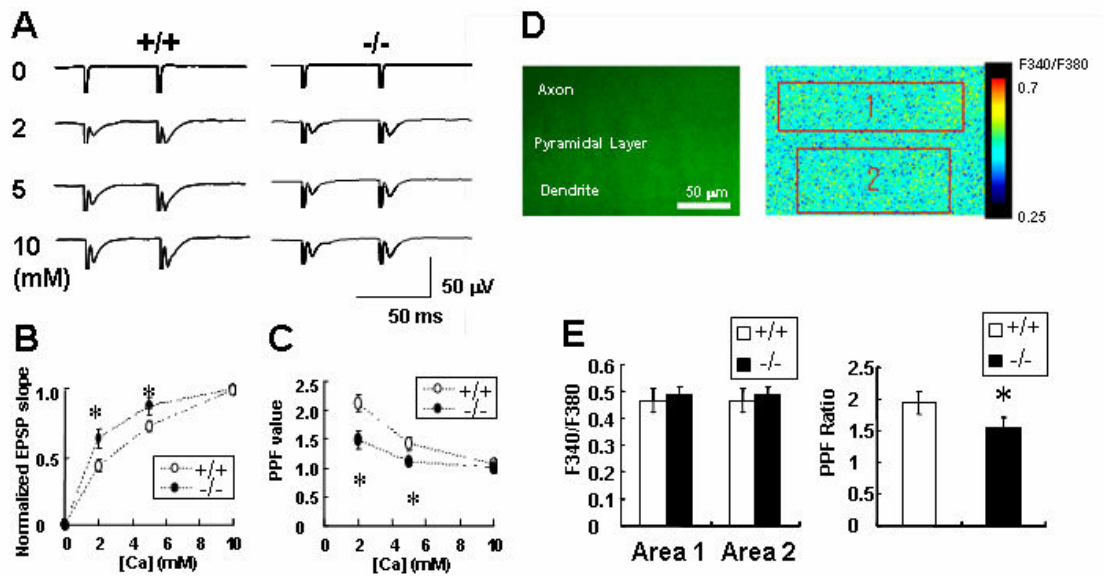

Fig. S8 Extracellular Ca^{2+} concentration-dependency of field-EPSP (fEPSP) from the hippocampal CA1 region in WT and SCR-KO mice.

(A) fEPSP response of WT and SCR-KO mice recorded under different concentrations of extracellular Ca^{2+} (0, 2, 5, and 10 mM) (trace is average of five recordings). (B) Extracellular Ca^{2+} concentration dependency of fEPSP slope (fEPSP slope was normalized to 1 under 10 mM extracellular Ca^{2+} concentration). (C) Extracellular Ca^{2+} concentration dependency of PPF value (stimulus interval: 50 ms). * $p < 0.05$, Student's *t*-test. +/+, wild-type; -/-, SCR-KO. (D) An example of the fluorescence image of SCR-KO hippocampal slice with Fura-2/AM. (left) Image of hippocampal slice excited by 340 nm laser, the scale bar is 50 μm; (right) same image with F340/F380 ratio encoded in pseudo-color. Area 1 (area containing axons of CA1 pyramidal cells); Area 2 (area containing dendrites of CA1 pyramidal cells and axon terminal of CA3 pyramidal cells). (E) Intracellular concentration of Ca^{2+} (F340/F380 ratios coded in pseudo-color as shown in (D)) were not altered in the hippocampal slice of the SCR-KO mice. Data show the mean ± SEM (n=5) (left column); the alteration of PPF ratios of the subsequent and initial fEPSP slopes (interpulse interval: 50 ms) recorded from hippocampal slices of WT or SCR-KO mice. Data show the mean ± SEM (n=5) (right column). * $p < 0.05$, Student's *t*-test. +/+, WT; -/-, SCR-KO. Basal intracellular Ca^{2+} concentration in SCR-KO neurons is within normal range.

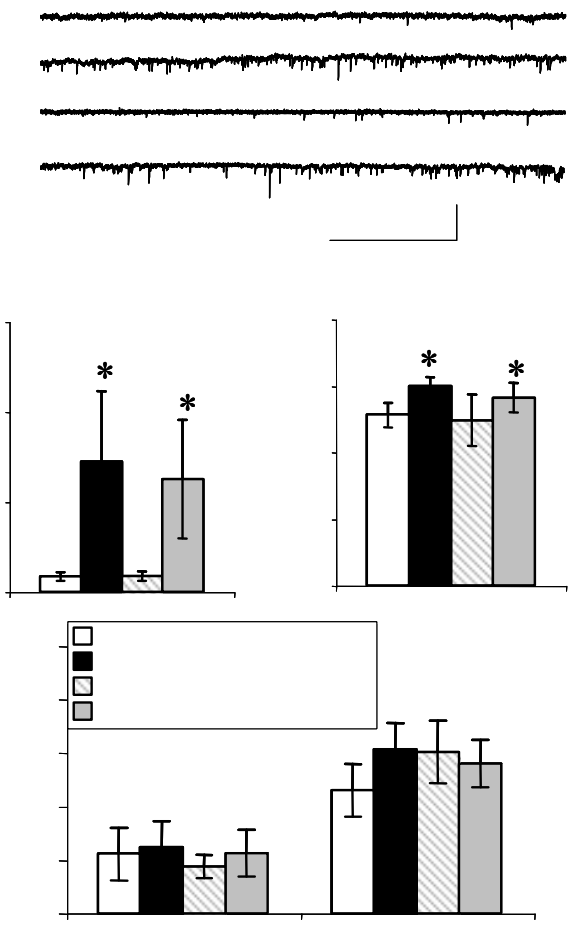

Fig. S9 Proteasome inhibitor MG132 affects the mEPSC but the calpain inhibitor does not.

Application of MG132 (50 μM) to primary cultured hippocampal neurons causes an increase in frequency and amplitude of mEPSC within 60 min. In contrast, neither amplitude nor frequency of mEPSC was altered following treatment of neurons with the calpain inhibitor ALLM.

(A) Representative traces of the mEPSC from primary cultured hippocampal neuron with or without MG132 treatment (50 μM, 1 hr) and/or Calpain inhibitor (Cal-Inhi, ALLM, 20 μM, 1 hr). The frequency of mEPSC was largely increased by the MG132 but not by the Calpain Inhibitor. (B) The mEPSC amplitude, rise time, and decay time. The amplitude was slightly increased and the rise and decay time were not changed by the MG132 treatment (50 μM, 1 hr). Data show the mean ± SEM (n=4). * $p < 0.05$, Student's t-test .

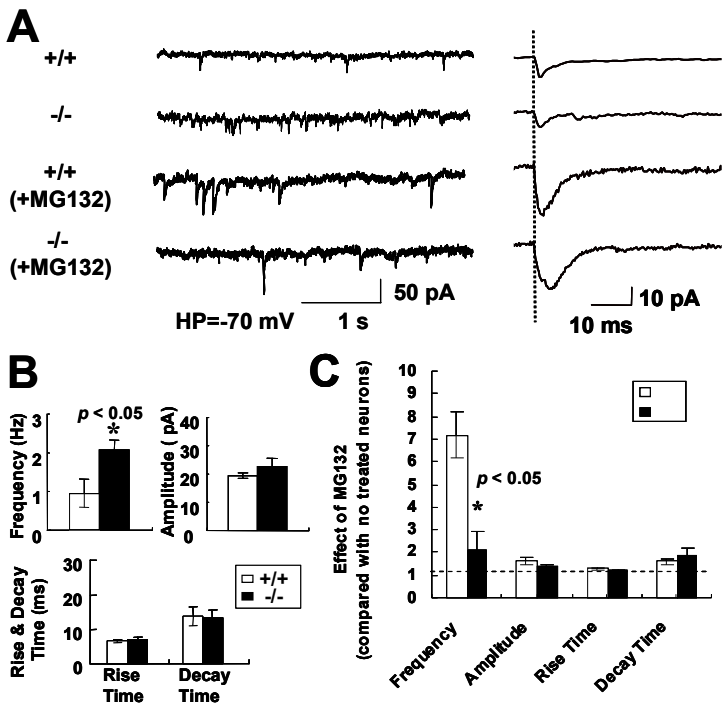

Fig. S10 AMPA receptor-mediated mEPSC from the primary cultured neuron.

The increase in mEPSC frequency by proteasome inhibitor and the poor response to MG132 in SCR-KO neurons were demonstrated in the dissociation cultures (7.2-fold in WT to 2.1-fold in SCR-KO) as well as acute slices.

(A) AMPA receptor-mediated mEPSC was recorded from cultured hippocampal CA1 pyramidal neurons of SCR-KO mice (with or without MG132 [50 μM, 1 hr] treatment) under voltage clamp conditions (HP = -70 mV). Representative mEPSC trace for 4 sec (left column); averaged mEPSC trace (right column). (B) The frequency of mEPSC was significantly increased in the SCR-KO mouse compared to the WT. The amplitude, rise and decay time did not show a significant difference between the WT and SCR-KO mice. * $p < 0.05$, Student's *t*-test. (C) Effect of MG132 (50 μM, 1 hr) on mEPSC parameters (Frequency, Amplitude, Rise Time and Decay Time) from cultured neurons of WT and SCR-KO mice. Data show the mean ± SEM (n=4). * $p < 0.05$, Student's *t*-test.